

Magnetic-field-induced reorientation in thin antiferromagnetic films: Spin-flop transition and surface-induced twist effects

A. N. Bogdanov* and U. K. Röbber†

Leibniz-Institut für Festkörperforschung und Werkstoffforschung Dresden, Postfach 270116, D-01171 Dresden, Germany

(Received 8 May 2003; published 16 July 2003)

Phenomenological equations for antiferromagnetic structures in a thin antiferromagnetic layer are derived and investigated in a broad range of magnetic fields and layer thicknesses. Corresponding phase diagrams magnetic field vs layer thickness are presented. Depending on thickness and values of the intrinsic and surface-induced interactions, the spin-flop transition occurs either as first-order transition (similar as in bulk materials) or continuously via twisted structures that are inhomogeneous across the layer thickness. The antiferromagnetic twisted phases have the same physical nature and display similar properties as spatially modulated phases observed in confined liquid crystals (Freedericksz effect) or in thin ferromagnetic films and multilayers.

DOI: 10.1103/PhysRevB.68.012407

PACS number(s): 75.50.Ee, 75.10.-b, 75.30.Kz, 75.70.-i

Magnetic nanostructures with antiferromagnetic interactions constitute a vast class of systems that currently are intensely investigated.^{1,2} They include various ferromagnetic/antiferromagnetic bilayers,^{2,3} synthetic antiferromagnets for spin valves and other applications,⁴ and ferromagnetic multilayers with antiferromagnetic coupling via spacer layers.^{5,6} In these composite structures the surfaces and interfaces substantially modify electronic and magnetic properties of the magnetic constituents compared to their bulk “states.” This causes a number of remarkable phenomena and effects as exchange bias, strongly enhanced uniaxial anisotropy and magnetoresistance, magnetic modulations, and others.² In particular, modern scanning and depth-resolving techniques^{2,7} reveal a strong modification of antiferromagnetic structures in ferro/antiferromagnetic bilayers.⁸ On the other hand, reorientation effects in the antiferromagnetic subsystems influence values of bias fields and induced anisotropy.⁹ These findings show that detailed investigations of magnetic states in the antiferromagnetic constituents of these nanosystems are crucial for an understanding of their properties. From theoretical side, only few results have been obtained for selected models, mostly by numerical means, see, e.g. Ref. 10. Contrary to the case of ferromagnetic nanostructures, there has been no consistent theoretical approach to the magnetic states in confined antiferromagnetic systems. In this Brief Report, we develop a phenomenological theory to provide an exhaustive description of magnetic states and of the main features of magnetization processes in antiferromagnetic nanolayers. We demonstrate important connections with bulk antiferromagnetism and with properties of other ordered media in confining geometries.

For definiteness, let us consider a thin antiferromagnetic layer of thickness D with uniaxial anisotropy sandwiched between nonmagnetic spacers. The layer is assumed to be infinite in x and y directions and bounded by parallel surfaces at $z = \pm D/2$. Employing a general phenomenological approach for the magnetism in nanostructures,¹¹ we start from the energy of a bulk and then adapt it for antiferromagnetic nanostructures by introducing extra energy-terms to describe modifications due to the surfaces. Within a continuum approach the magnetic energy density for a bulk, two-

sublattice, uniaxial antiferromagnet can be written in the following form:¹²

$$w = \alpha [(\partial \mathbf{m}_1)^2 + (\partial \mathbf{m}_2)^2] + \alpha' (\partial \mathbf{m}_1 \partial \mathbf{m}_2) + e(\mathbf{m}_1, \mathbf{m}_2), \quad (1)$$

where \mathbf{m}_i are unity vectors along the sublattice magnetization (we neglect here paraproceses which are important near the ordering temperature only), (α, α') are constants of inhomogeneous exchange interactions, and $\partial \mathbf{m}_i \equiv \sum_k (\partial \mathbf{m}_i / \partial x_k)$. The homogeneous part of the energy density $e = [\lambda \mathbf{m}_1 \cdot \mathbf{m}_2 - \mathbf{H} \cdot (\mathbf{m}_1 + \mathbf{m}_2) + e_a]$ includes homogeneous exchange coupling (λ), the interaction energy with the magnetic field \mathbf{H} and the anisotropy e_a . In most known bulk antiferromagnetic crystals in attainable magnetic fields $\lambda \gg e_a, |\mathbf{H}|$, and the leading anisotropy is a uniaxial term with respect to an axis \mathbf{a} . In terms of staggered magnetization $\mathbf{l} = (\mathbf{m}_1 - \mathbf{m}_2)/2$ and total magnetization $\mathbf{m} = (\mathbf{m}_1 + \mathbf{m}_2)/2$, it can be written as $e_a = -B_1(\mathbf{l} \cdot \mathbf{a})^2 - B_2(\mathbf{l} \cdot \mathbf{a})^4 - (2\beta - B_1)(\mathbf{m} \cdot \mathbf{a})^2$ ($B_1, \beta \gg B_2$).¹² For $B_1 > 0$ the direction of the easy magnetizations (easy axis) coincides with the \mathbf{a} axis, and the energy functional w (1) can be reduced to the following form (for details, see Ref. 12): $w = A(\partial \theta)^2 + B_1 \Phi(\theta)$ with $A = \alpha + \alpha'$ and

$$2\Phi(\theta) = -K \cos^2 2\theta + a \cos 2\theta + b \sin 2\theta,$$

$$K = (B_2/B_1 + \beta/\lambda)/2, \quad a = h_{\parallel}^2 - h_{\perp}^2 - 1,$$

$$b = 2h_{\parallel}h_{\perp}, \quad \mathbf{h} = \mathbf{H}/H_{\text{SF}}, \quad H_{\text{SF}} = 2\lambda B_1. \quad (2)$$

The variable θ is the angle between \mathbf{a} axis and \mathbf{l} , and H_{SF} is a spin-flop field. For equilibrium states \mathbf{m}_i is in the plane spanned by easy axis \mathbf{a} and external field \mathbf{h} . The component of the field in direction of \mathbf{a} is denoted by h_{\parallel} , the transverse component is h_{\perp} . For $K > 0$ at a field $h_{\parallel} = 1, h_{\perp} = 0$ ($a = 0, b = 0$) the spin-flop transition takes place, i.e., a phase transition between antiferromagnetic (AF) phase with $\theta = 0$ and spin-flop (SF) phase with $\theta = \pi/2$. Note that in the vicinity of the spin-flop transition, where a and b are anomalously small, the term proportional to K in Eq. (2) plays the dominant role in the energy balance.

In confined systems, their surfaces/interfaces induce additional magnetic interactions. They can be described by additional energy contributions in the form $e_s(\mathbf{r}) = \eta(\mathbf{r})\Xi(\mathbf{m}_i)$ where $\Xi(\mathbf{m}_i)$ are invariants describing exchange, anisotropic, or other interactions, $\eta(\mathbf{r})$ are spatially inhomogeneous coefficients that should be treated as internal variables similar to the magnetization fields $\mathbf{m}_i(\mathbf{r})$.¹¹ The equilibrium distributions of $\mathbf{m}_i(\mathbf{r})$ and such induced “fields” $\eta(\mathbf{r})$ are derived by minimization of the energy functional (1) and interaction functionals for $\eta(\mathbf{r})$ with appropriate boundary conditions (for examples, see Ref. 11). For an antiferromagnetic layer the fields $\eta(\mathbf{r})$ may include surface-related counterparts of bulk exchange and anisotropy constants $\lambda_s(z), B_{1s}(z), B_{2s}(z), \beta_s(z)$ which, in homogeneous layers, vary only along the normal to the layer. Here, we simplify this general framework. The induced fields $\eta(z)$ have strongly pronounced surface character and decay exponentially fast into the depth of the layer.¹¹ Thus, integration transforms energy contributions $e_s(z)$ into a sum of surface energies with constant coefficients $\int_{-D/2}^{D/2} e_s(z) dz = \sum_{i=1}^2 \tilde{\eta}^{(i)} \Xi(\mathbf{m}_i)|_{z=\pm D/2}$.

Hence, the surface induced exchange and anisotropy energy contributions are reduced to surface terms with constant coefficients $\tilde{\lambda}^{(i)}, \tilde{B}_1^{(i)}, \tilde{B}_2^{(i)}$, and $\tilde{\beta}^{(i)}$ ($i=1,2$). By introducing a new length $z=L_0\xi$, $d=D/L_0$ ($L_0=\sqrt{A/B_1}$ is exchange length¹²) and by scaling energy as $\tilde{W}=W/\sqrt{AB_1}$, the energy of the antiferromagnetic layer can be written as

$$\tilde{W} = \int_{-d/2}^{d/2} [(d\theta/d\xi)^2 + \Phi(\theta)] d\xi + \Omega^{(1,2)}|_{\xi=\pm d/2}, \quad (3)$$

where the surface energies $\Omega^{(i)}(\theta)$ are

$$\begin{aligned} 2\Omega^{(i)}(\theta) &= -\tilde{K}_i \cos^2 2\theta + \tilde{a}_i \cos 2\theta + \tilde{b}_i \sin 2\theta, \\ \tilde{a}_i &= -\kappa^{(i)}(h_{\parallel}^2 - h_{\perp}^2) - \nu^{(i)}, \quad \tilde{b}_i = -2\kappa^{(i)}h_{\parallel}h_{\perp}, \\ 2\tilde{K}_i &= (\tilde{B}_2^{(i)}/B_1 + \tilde{\beta}^{(i)}/\lambda)/L_0. \end{aligned} \quad (4)$$

Here, the ratios of surface energies to bulk energies $\kappa^{(i)} = \tilde{\lambda}^{(i)}/(\lambda L_0)$ and $\nu^{(i)} = \tilde{B}_1^{(i)}/(B_1 L_0)$ and the parameters \tilde{K}_i depend on the properties of individual surfaces. They are free (phenomenological) parameters of the theory, together with “bulk” phenomenological constants A , K , and H_{SF} . Energy (3) is valid for arbitrary orientation of the easy axis \mathbf{a} within the layer.

Twisted phases. For the surface energies $\Omega^{(i)}(\theta)$ (4) the conditions of the spin-flop transition ($\tilde{K}_i > 0$, $\tilde{a}_i = 0$, $\tilde{b}_i = 0$) do not coincide with those for the bulk spin flop (1). Thus, in a certain range of fields the volume and surface interactions favor different magnetic configurations. This competition may distort the homogeneous, collinear ordering and can stabilize inhomogeneous phases with continuous rotation of the vector \mathbf{l} across the film thickness. The occurrence of such *twisted* states under pinning (or anchoring) influence of the surfaces is a rather general effect and has been observed in a number of condensed matter systems. Initially, these surface-induced distortions have been identified in nematics (Freed-

ericksz transition¹³). Later different twisting effects have been observed and thoroughly investigated in many classes of liquid crystals and form the physical basis for all liquid-crystal display technologies.¹⁴ In ferromagnetic structures twisted phases are caused by the competition between surface exchange or anisotropy energies and volume anisotropies or the interaction with applied magnetic field.¹⁵ Spiraling in exchange spring magnets and exchange bias systems also belongs to this class of phenomena.² The energy functional (3) has a similar mathematical structure as those for confined liquid crystals¹⁴ [for $h_{\perp}=0$ it even coincides] and ferromagnetic thin layers.¹⁵ Hence, we have reduced the problem of the inhomogeneous states in confined antiferromagnets to the mathematically equivalent and well-studied problem of twisted states in liquid crystals and ferromagnetic nanostructures. In our work, this is the central point which provides a general solution for the magnetic behavior, including noncollinear magnetic states, of antiferromagnetic layers. However, compared to these known twist effects, those in confined antiferromagnets should display a large variability and a strong dependency on the applied field and the materials parameters of the system. This is due to peculiarities of the antiferromagnetic ground states near the spin-flop transition¹² and the particular, field-dependent form of the “anchoring” energy (4).

We discuss some general features of these twisted phases in an antiferromagnetic layer with identical surfaces given by $\tilde{K}_i = \tilde{K}$, $\kappa^{(i)} = \kappa$, $\nu^{(i)} = \nu$, for $i=1,2$ in a field directed along the easy axis $h \equiv h_{\parallel}$, $h_{\perp} = 0$. The AF (SF) phase, respectively, is stable for negative (positive) values of

$$\tilde{a}_0 = -|\kappa|[\text{sgn}(\kappa)h^2 + \text{sgn}(\nu)h_0^2], \quad h_0 = \sqrt{|\nu/\kappa|}. \quad (5)$$

The critical fields for the transitions between twisted phase and the homogeneous states can be calculated by expansion of the functional (3) for $\theta \ll 1$ (AF phase) and $(\pi/2 - \theta) \ll 1$ (SF phase) and can be reduced to the following expressions:

$$d_{1,2} = \Pi_{\pm}(h) \text{arcth}[\Lambda_{\pm}(h)], \quad d_{3,4} = \Pi_{\pm}(h) \text{arctg}[\Lambda_{\pm}(h)] \quad (6)$$

with $\Pi_{\pm}(h) = 2/\sqrt{|1-h^2 \pm K|}$ and $\Lambda_{\pm} = |\tilde{a}_0 \mp \tilde{K}|/\sqrt{|1-h^2 \pm K|}$ where the upper (lower) signs are for the AF (SF) phases, respectively. The pinning effects of the surface interactions Eq. (6) lead to inhomogeneous distribution of the magnetization in the spin-flop phase. Such states are known from investigations on discretized models.¹⁶ Depending on the sign of the parameters κ , ν , and values of K and \tilde{K} a number of different scenarios can be realized. We illustrate this by selected thickness vs field phase diagrams that reflect the evolution of twisted states (Figs. 1, 2). For negative values of κ and ν the surface energy favors SF phase for arbitrary values of the applied field. Then, the twisted phase exists in the interval $[d_1(h), d_4(h)]$ below the bulk spin-flop field (Fig. 1). The values $d_1(0)$, $d_4(0)$ (6) determine the thickness interval where the twisted phase exists at zero field. For $\Lambda_-(0) > 1$ the AF phase is always unstable and the twisted phase corresponds to the ground states for all thicknesses $d > d_4(0)$. For $\kappa < 0$, $\nu > 0$ and $h_0 > 1$ the twisted

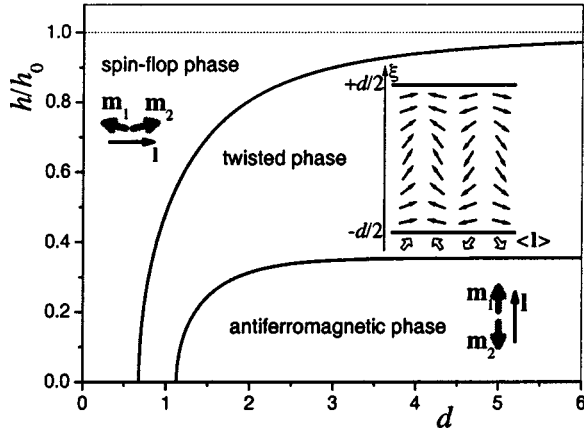


FIG. 1. Example of phase diagram for magnetic states in an antiferromagnetic layer with field h in direction of easy axis \mathbf{a} vs thickness d for $\kappa < 0$, $\nu < 0$. [d in units of exchange length L_0 , and h_0 is the spin-flop field defined in Eq. (5)]. Inset: magnetic structure [staggered vector $\mathbf{I}(\xi)$] in the layers for the four degenerate realizations of the twisted phase (arbitrarily $\mathbf{a} \parallel \xi$). Open arrows are average staggered vectors $\langle \mathbf{I} \rangle = \int_{-d/2}^{d/2} \mathbf{I}(\xi) d\xi$.

phase is realized in the range $[d_3(h), d_4(h)]$ above the bulk spin-flop field (Fig. 2). The equilibrium structures $\theta(z)$ in the twisted phase can be calculated by minimizing the layer energy (3) with the boundary conditions $8A\lambda(d\theta/dz) = \pm(\partial\Omega^{(1,2)}/\partial\theta)$ for $\xi = \pm d/2$. They describe the continuous evolution of the twisted states from AF to SF configuration (see analysis of similar solutions for liquid crystals systems in Ref. 14). Sufficiently large values of K and \tilde{K} may suppress the twisted phase. In this case, the transition between the homogeneous states is determined by the minima of energy $\tilde{W} = \Phi(\theta)d + \Omega^{(1)}(\theta) + \Omega^{(2)}(\theta)$ which is derived by integration in Eq. (3). Because energy \tilde{W} functionally coincides with that of the bulk antiferromagnet $\Phi(\theta)$ (2) the surface/interface effects in this case can be taken into ac-

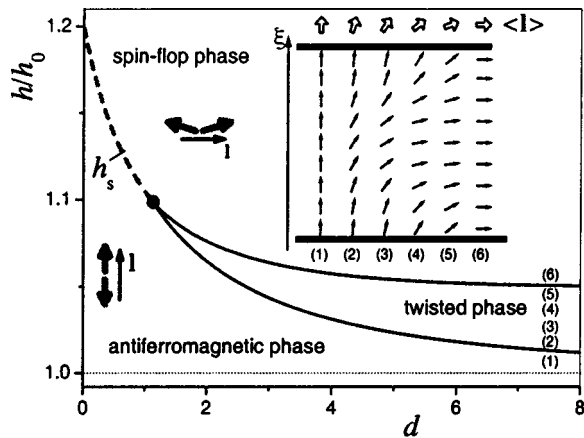


FIG. 2. Phase diagram as Fig. 1, but for $\kappa < 0$, $\nu > 0$. For d below the tricritical point \bullet , the transition from antiferromagnetic to spin-flop phase is first-order [dashed line $h_s(d)$, Eq. (7)]. A continuous evolution via the twisted phase occurs for larger d . Inset: magnetic structures [staggered vector $\mathbf{I}(\xi)$] with increasing field h corresponding to the points (1) – (6).

count by the following redefinition of the coefficients in $\Phi(\theta)$ (2) $a \rightarrow a_s = h_{\parallel}^2 - h_{\perp}^2 - h_s^2(d)$, $b_s = b$, $K \rightarrow K_s$, where

$$K_s = \frac{K + (\tilde{K}_1 + \tilde{K}_2)/d}{1 - (\kappa^{(1)} - \kappa^{(2)})/d}, \quad h_s = \sqrt{\frac{1 + (\nu^{(1)} + \nu^{(2)})/d}{1 - (\kappa^{(1)} + \kappa^{(2)})/d}}. \quad (7)$$

This result is an analogue to Néel's formula for effective anisotropy of a magnetic layer with surface anisotropy.¹ The transition between AF and SF occurs at the critical field $h_s(d)$ (7) as a first-order process without intervening twisted phase. In thickness vs field phase diagrams, these two types of SF transitions are separated by a tricritical point (Fig. 2).

The degeneracy of states in the magnetic twisted phases (inset Fig. 1) leads to specific multidomain structures.¹¹ The magnetization processes in the twisted phases are determined (i) by the continuous evolution of spin configurations in the twisted phases and (ii) by expansion of certain domain types at the expense of others, similarly to domains in ferromagnetic twisted phases.¹¹ In the case of suppressed twisted phases, the first-order transition from the AF to SF phase also occurs via thermodynamically stable multidomain structures.¹² Both types of transitions have qualitatively similar magnetization curves or generally macroscopic magnetic properties. Thus, special experimental approaches are necessary to detect differences between such states and to identify them.

The first-order transition exists in close vicinity of the spin-flop field [$h_{\parallel} = h_s(d)$, $h_{\perp} = 0$]. For $h_{\parallel} = h_s(d)$ the difference between the competing homogeneous phases is reduced from $\Delta\theta = \pi/2$ for $h_{\perp} = 0$ to zero at $h_{\perp} = K_s(d) \ll 1$. Correspondingly, all magnetization processes near the spin-flop transition strongly depend on the orientation and homogeneity of the applied magnetic field.

In magnetic nanostructures, the surface-related magnetic interactions strongly differ from bulk values and can be manipulated in a broad range by various physical and chemical factors.¹ Thus, one may expect that the theoretical scenarios of the different phase diagrams (Figs. 1, 2) can be realized in experimental antiferromagnetic nanosystems. Nanosized layers of antiferromagnets such as MnF_2 , FeF_2 and bilayers such as Fe/MnF_2 , Fe/FeF_2 (Refs. 8,9) should be good candidates to investigate evolution of these antiferromagnetic states. In particular, the here established relations between parameters of the magnetic surface-energy contributions and equilibrium antiferromagnetic configurations provide means to determine values of bias fields and other surface induced interactions from experimental observations of reorientation effects in an antiferromagnetic layer or sublayer.

In Ref. 17, it was shown that the continuum and discretized models quantitatively agree even for few magnetic layers for functionals of type (3). In this connection, magnetic superlattices consisting of a finite number of ferromagnetic nanolayers with antiferromagnetic couplings (e.g., Fe/Cr superlattices^{5,6}) deserve special consideration. Up to now, such layered systems have been theoretically investigated by a simple one-dimensional discretized model.¹⁸ In continuum limit this model is equivalent to functional (3) with $K = \tilde{K}_i = 0$ and $h_0 = 1/\sqrt{2}$. Due to specially chosen and

fixed parameters, the results of Ref. 18 do not comprise most of the physical states and phase diagrams revealed by our theory. However, a theoretical analysis of this model shows that the interplay of an intermediate uniaxial anisotropy and cut exchange bonds at the boundaries of such stacked systems stabilizes a number of different spatially inhomogeneous states unknown in other types of magnetic nanostructures.¹⁹ Recent experiments confirm the complex character of magnetic states in these systems.^{5,6} Spatially inhomogeneous structures have been observed in Ref. 5, while other authors find a direct transition between AF and SF phase similar to that in bulk materials.⁶ The development of the continuum theory together with further investigations on

generalized discretized models should give a deeper insight into these unconventional systems and indicate the range of parameters where the continuum model can be applied.

In conclusion, we stress that, as its derivation relies only on elementary notions and properties of antiferromagnetic materials, the phenomenological theory (3), gives a consistent and general description of magnetic states in antiferromagnetic nanolayers. It provides also the basis for detailed micromagnetic investigations of antiferromagnetic nanostructures within the standard phenomenological theory of magnetism.²⁰

A. N. B. thanks H. Eschrig for support and hospitality at the IFW Dresden.

*Permanent address: Donetsk Institute for Physics and Technology, 340114 Donetsk, Ukraine. Electronic address: bogdanov@kinetic.ac.donetsk.ua

†Electronic address: u.roessler@ifw-dresden.de

¹P. Moriarty, Rep. Prog. Phys. **64**, 297 (2001); S.D. Bader, Surf. Sci. **500**, 172 (2002); L. Néel, J. Phys. Radium **15**, 225 (1954); M.T. Johnson, P.J.H. Bloemen, F.J.A. den Broeder, and J.J. de Vries, Rep. Prog. Phys. **59**, 1409 (1996).

²A.E. Berkowitz and K. Takano, J. Magn. Magn. Mater. **200**, 552 (1999).

³M.R. Fitzsimmons *et al.*, Phys. Rev. Lett. **84**, 3986 (2000); C. Leighton *et al.*, *ibid.* **86**, 4394 (2001).

⁴G.J. Strijkers, S.M. Zhou, F.Y. Yang, and C.L. Chien, Phys. Rev. B **62**, 13 896 (2000).

⁵P. Steadman *et al.*, Phys. Rev. Lett. **89**, 077201 (2002); S.G.E. te Velthuis, J.S. Jiang, S.D. Bader, and G.P. Felcher, *ibid.* **89**, 127203 (2002); V. Lauter-Pasyuk *et al.*, *ibid.* **89**, 167203 (2002).

⁶K. Temst *et al.*, Physica B **276-278**, 684 (2000); D.L. Nagy *et al.*, Phys. Rev. Lett. **88**, 157202 (2002).

⁷M.R. Freeman and B.C. Choi, Science **294**, 1484 (2001); O. Pietzsch, A. Kubetzka, M. Bode, and R. Wiesendanger, Phys. Rev. Lett. **84**, 5212 (2000); A. Scholl *et al.*, Science **287**, 1014 (2000).

⁸J. Nogues, D. Lederman, T.J. Moran, and I.K. Schuller, Phys. Rev. Lett. **76**, 4624 (1996); H. Ohldag *et al.*, *ibid.* **86**, 2878 (2001).

⁹F. Nolting *et al.*, Nature (London) **405**, 767 (2000); J. Nogues *et al.*, Phys. Rev. B **61**, R6455 (2000).

¹⁰N. Cramer and R.E. Camley, Phys. Rev. B **63**, 060404 (2001); A.S. Carriço, R.E. Camley, and R.L. Stamps, *ibid.* **50**, 13 453 (1994).

¹¹A.N. Bogdanov and U.K. Rößler, Phys. Rev. Lett. **87**, 037203 (2001); A.N. Bogdanov, U.K. Rößler, and K.-H. Müller, J. Magn. Magn. Mater. **238**, 155 (2002).

¹²For a review on main physical effects in bulk uniaxial antiferromagnets, see V.G. Bar'yakhtar, A.N. Bogdanov, and D.A. Yablonskii, Usp. Fiz. Nauk. **156**, 47 (1988) [Sov. Phys. Usp. **31**, 810 (1988)], and references cited therein.

¹³V. Fredericksz and V. Zolina, Trans. Faraday Soc. **29**, 919 (1933); H. Zocher, *ibid.* **29**, 945 (1933).

¹⁴P.G. de Gennes and J. Prost, *The Physics of Liquid Crystals* (Clarendon, Oxford, 1993).

¹⁵E. Goto, N. Hayashi, T. Miyashita, and K. Nakagawa, J. Appl. Phys. **36**, 2951 (1965); A. Thiaville and A. Fert, J. Magn. Magn. Mater. **113**, 161 (1992).

¹⁶F. Keffer and H. Chow, Phys. Rev. Lett. **31**, 1061 (1973); F.C. Nörtemann, R.L. Stamps, A.S. Carriço, and R.E. Camley, Phys. Rev. B **46**, 10 847 (1992).

¹⁷X. Hu, R. Tao, and Y. Kawazoe, Phys. Rev. B **54**, 65 (1996).

¹⁸D.L. Mills, Phys. Rev. Lett. **20**, 18 (1968); R.W. Wang *et al.*, *ibid.* **72**, 920 (1994); M. Momma and T. Horiguchi, Physica A **259**, 105 (1998).

¹⁹U.K. Rößler and A.N. Bogdanov (unpublished).

²⁰A. Hubert and R. Schäfer, *Magnetic Domains* (Springer-Verlag, Berlin, 1998).